Imino-tetrahydro-benzothiazole Derivatives as p53 Inhibitors: Discovery of a Highly Potent in Vivo Inhibitor and Its Action Mechanism

Nicolas Pietrancosta,[†,‡] Anice Moumen,[†] Rosanna Dono,[†] Paul Lingor,[§] Veronique Planchamp,[§] Fabienne Lamballe,[†] Mathias Bähr,[§] Jean-Louis Kraus,*[,†,‡,||] and Flavio Maina*[,†,||]

Developmental Biology Institute of Marseille (Université. de la Mediterranée), Inserm UMR623 (CNRS - INSERM) Campus de Luminy-Case 907, Marseille Cedex 09, France, Laboratoire de Chimie Biomoléculaire (Université. de la Mediterranée), Campus de Luminy-Case 907, Marseille Cedex 09, France, and Department of Neurology, University of Göttingen, Waldweg 33, 37075 Göttingen, Germany

Received March 20, 2006

Several neurological disorders manifest symptoms that result from the degeneration and death of specific neurons. p53 is an important modulator of cell death, and its inhibition could be a therapeutic approach to several neuropathologies. Here, we report the design, synthesis, and biological evaluation of novel p53 inhibitors based on the imino-tetrahydrobenzothiazole scaffold. By performing studies on their mechanism of action, we find that cyclic analogue **4b** and its open precursor **2b** are more potent than pifithrin-α (**PFT**-α), which is known to block p53 pro-apoptotic activity in vitro and in vivo without acting on other pro-apoptotic pathways. Using spectroscopic methods, we also demonstrate that open form **2b** is more stable than **4b** in biological media. Compound **2b** is converted into its corresponding active cyclic form through an intramolecular dehydration process and was found two log values more active in vivo than **PFT**-α. Thus, **2b** can be considered as a new prodrug prototype that prevents in vivo p53-triggered cell death in several neuropathologies and possibly reduces cancer therapy side effects.

Introduction

Neurodegenerative disorders, such as stroke, Alzheimer's, and Parkinson's disease, manifest symptoms of degeneration and progressive loss of specific neuron populations.[1−3] Whereas different neuronal subpopulations are affected in each of these pathologies, the biochemical and cellular events leading to neuronal dysfunction and cell death share a common final cascade, which involves increased oxidative stress, the disruption of calcium homeostasis, and the activation of an intrinsic apoptotic program.[3,4] The activation of the tumor suppressor gene p53 plays a crucial role in regulating the death of neurons in vitro, following apoptotic stimuli involving molecules such as glutamate or DNA-damaging agents.[5−8] Studies of p53-deficient mice have confirmed the essential role of p53 in neuronal apoptosis caused by ischemic and excitotoxic insults.[6,9] In vivo evidence of p53 implication in neuronal death has also been reported in stroke,[10,11] traumatic brain injury,[12] and Alzheimer's disease.[13] The biological function of p53 is largely mediated through the transactivation of specific target genes, such as p21, Bax, and PUMA.[14] Moreover, p53 promotes apoptosis by preventing the expression of survival genes, by interference with the activity of specific transcription factors, or by regulating the mitochondrial translocation of Bax.[15]

The involvement of p53 in neuronal death raises the possibility that p53 inhibitors might prove effective in suppressing the degenerative processes in neurodegenerative disorders. The antiparasitic compound, **PFT**-α (Figure 1) has been identified for its ability to protect cells against radiation, excitotoxic, and amyloid-induced neuronal death.[16]

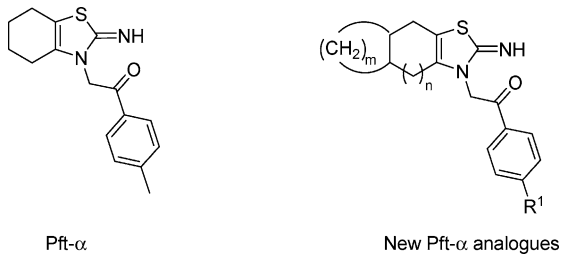

Figure 1. Structure of Pifithrin-α (**PFT-α**) and the general structure of related analogues.

Moreover, **PFT**-α protects cultured hippocampal neurons against death induced by DNA-damaging agents.[17,18] **PFT**-α prevents cell death by inhibiting p53 transcriptional activity, mitochondrial damage, and caspase activation, whereas it has no effects on p53 protein levels and phosphorylation.[17] Its specificity to block p53 has been proven by its failure to prevent p53-independent cell death.[17] Recent in vivo studies further emphasized the potential of **PFT**-α in preventing neuronal death and delaying neurodegeneration.[17−19] On the basis of these observations, the identification of more potent chemical compounds able to efficiently inactivate p53 activity and an understanding of their action mechanism are promising contributions to neurodegenerative disease progression. Some compounds based on the **PFT**-α scaffold and their preliminary biological activities have already been published by our group,[20] and some other compounds described by Bachechath have been reported as inhibitors of apoptosis in Lymphocytes.[21] In this article, we report the complete synthesis of all of the p53 inhibitors, their unique specific neuroprotective activity through p53 inhibition, and their action mechanism in vitro and in vivo.

Chemistry

We sought to develop novel p53 inhibitors able to efficiently block p53 pro-apoptotic activity both in vitro and in vivo. Although the similarity property principle states that structurally

* Corresponding author. Tel: +33 491 82 9141. Fax: +33 491 82 9416. E-mail: kraus@ibdm.univ-mrs.fr (J.-L.K.). E-mail: maina@ibdm.univ-mrs.fr (F.M.).

† Developmental Biology Institute of Marseille (Université. de la Mediterranée).

‡ Laboratoire de Chimie Biomoléculaire (Université. de la Mediterranée).

§ University of Göttingen.

|| These authors contributed equally to this work.

10.1021/jm060318n CCC: $33.50
Published on Web 05/24/2006

Scheme 1[a]

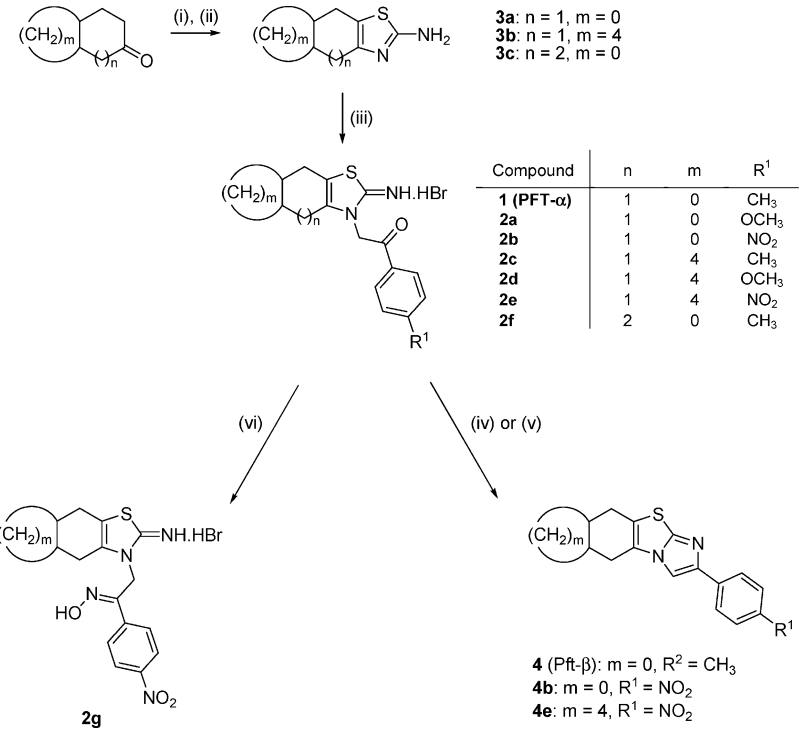

[a] (i) Thiourea, I_2, 110 °C, 12 h; (ii) saturated Na_2CO_3, H_2O; **1a** (52%), **1b** (47%), **1c** (37%), for 2 steps; (iii) 4-R^2-C_6H_4-C(O)-CH(R^1)Br, toluene, rt, 48 h; **PFT-α** *(54%)*, **2a** (61%), **2b** (55%), **2c** (80%), **2d** (41%), **2e** (47%), **2f** (40%); (iv) MeOH, rt; quantitative for **4b** and **4e**; (v) biological medium, 37 °C; quantitative for **4**, **4b**, **4e**; (vi) NH_2-OH, **2b**, CH_2Cl_2, 3 h; **2g** (35%).

similar compounds are expected to have similar activities,[22] small structural modifications can nevertheless produce either a slight modulation or a dramatic loss of activity. Therefore, considering the **PFT**-α scaffold as a privileged structure according to Evans' definition,[23] we introduced chemical modifications to generate a series of novel **PFT**-α analogues (Scheme 1).

The synthesis of 2-aminothiazole hydroiodide salt precursors was carried out according to the method described by King et al.[24] The solvent free reaction was performed by heating various cyclic ketones (cyclohexanone, 2-decalone, and cycloheptanone) with thiourea in the presence of iodine. Basic treatment of the hydroiodide salt allowed the isolation of the corresponding free aminothiazoles **3a**−**c**, which could be N-alkylated at the endocyclic N3-position by selected α-bromoacetophenones at room temperature in toluene. The resulting N3-substituted 2-iminothiazole derivatives **PFT-α** and **2a**−**g** were isolated in yields ranging from 40 to 70% after purification by crystallization.

Cyclic analogues were obtained from the open form simply by stirring nitro **PFT-α** analogues **2b** and **e** in protic solvents (EtOH, ^{i}PrOH). The corresponding tricyclic nitro derivatives **4b** and **e** resulting from a dehydration process were isolated in quantitative yields and fully characterized. Some of these derivatives have already been reported.[20,21] The ability of **PFT-α** analogues to undergo this dehydration process depends on the electron-donating or electron-withdrawing properties of the phenyl ring substituents. Compounds bearing withdrawing substituents such as a nitro group on the phenyl ring, for example, **2b** and **e**, were found to be more sensitive to the dehydration process (few hours at room temperature) than analogues bearing electron-donating substituents, which needed a longer time to cyclize (**2a**, **c**, **d**, **f**) (The cyclization process will be discussed in more detail below.) The new opened PFT analogues (**2a**−**f**), cyclic PFT analogues (**4a**−**g**) as well as oxime derivative **2g** were tested for their ability to block p53-induced death.

Results and Discussion

Cell-Based Assay in Vitro Evaluation. The compounds were submitted first to an in vitro cell-based assay as a primary screening. As the read-out system for p53 inhibitor screening, a survival assay was performed using primary cultures of E15.5 cortical neurons exposed to DNA-damaging agents (**PFT**-α being considered as a p53 reference inhibitor). Before screening the new analogues, we first verified that anticancer drugs etoposide or camptothecin induced the death of primary cortical neuron cultures in a time- and concentration-dependent manner as shown in Figure 2, and then, we ensured that cortical neuron-induced death was p53-dependent. For this purpose, primary cultures of *p53*$^{-/-}$ cortical neurons were submitted to etoposide treatment, and as expected (Figure 2), no death was observed after the etoposide treatment of these p53-mutated cortical neurons.

We next performed an assay to discover whether the new synthesized **PFT-α** analogues (**2a**−**g**, **4b**, **4e**) prevented cortical neuron death induced by etoposide (Figure 3).

As can be seen in Figure 3, tricyclic analogue **4b** (ED_{50} = 30nM) is one order magnitude more active than **PFT-α** in protecting cortical neurons exposed to etoposide. In contrast, the replacement of the cyclohexene ring by larger cycles (e.g., cycloheptene or octahydro-naphthalene: **2f** and **c**, respectively) abolished inhibitory effects, showing that ring size is determinative of activity. Moreover, the introduction of different substituents on the aromatic ring (**2a** and **e**) modulate their inhibitory activities. Interestingly, **2b**, the corresponding open form of the cyclic analogue **4b**, shows a p53 inhibitory activity similar to that of **PFT-α**, whereas oxime **2g** was found inactive in preventing p53-induced death. This later observation is of interest because oxime **2g** cannot be cyclized.

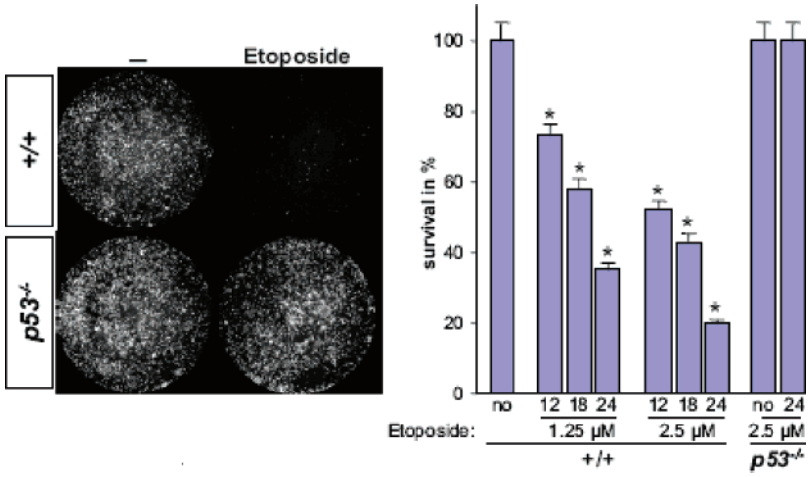

Figure 2. Survival of wild-type (+/+) and $p53^{-/-}$ mutant cells exposed to etoposide, evaluated in a time- and dose-dependent manner. Cortical neuron cultures without etoposide treatment are set to 100%. $p < 0.001$ (*).

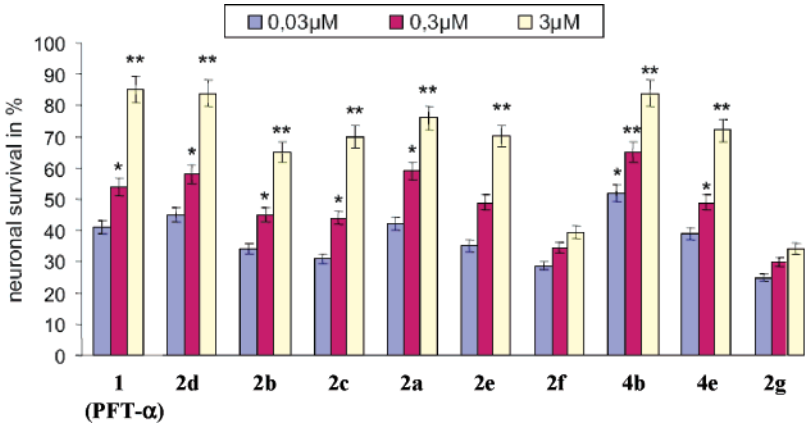

Figure 3. Percentage of survival effect of p53 inhibitors. None of the new derivatives were toxic at 10 μM. Cortical neuron cultures without etoposide treatment are set to 100%. Plots show means of at least six independent experiments, each performed in triplicate, with standard errors (sem). $p < 0.01$ (*) and $p < 0.001$ (**).

At this point, we selected analogue **2b** (open form) and its corresponding cyclic form **4b** as the most representative analogues for mechanistic biochemistry studies and in vivo activities.

Action Mechanism Studies. **Specificity of 4b Inhibitory Activity.** This primary screening allowed us to identify **4b** as the most efficient inhibitor of p53-triggered neuronal death in vitro. We first investigated whether **4b** would also affect p53-independent cell death. Knowing that the overexpression of a cytoplasmic fragment of the Met receptor tyrosine kinase ($p40^{Met}$) in cortical neurons induces apoptosis[25] in a p53-independent manner, we took advantage of this experimental system to test the action of **4b** and **PFT-α** (reference compound) on other pro-apoptotic pathways. Interestingly, **4b** and **PFT-α** did not prevent cortical neuronal death induced by $p40^{Met}$, showing the remarkable specificity in the inhibitory action of **4b** on p53 (Figure 4). In contrast to published results, which have shown that some PFT analogues prevent apoptosis in lymphocytes through both dependent and independent p53 pathways,[21] we found that the tested analogues were clearly p53-dependent inhibitors in our cortical neuron apoptosis assay.

p53 Posttranscriptional Activity of 4b. We next biochemically assayed the ability of compounds **2b**, **4b**, and **PFT-α** to antagonize p53 by testing p53 phosphorylation and the induction of its downstream target, p21/WAF1.

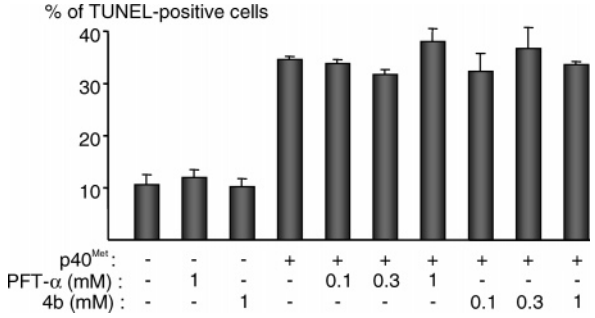

Figure 4. p53-independent death of cortical neurons was not prevented by **4b** treatment. Mouse embryonic cortical neurons were electroporated with either an empty vector (−) or with the pro-apoptotic fragment of Met tyrosine kinase receptor (p40Met) and then treated with either **PFT-α** or **4b** at indicated concentrations. Forty hours after transfection, TUNEL was performed, and the percentage of TUNEL-positive cells was determined. Results are the mean values of two independent experiments.

We found that etoposide treatment triggered p53 phosphorylation on the S_{15} residue [26] and the up-regulation of the p53 transcriptional target p21/WAF1[26,27] in wild-type cortical neurons but not in $p53^{-/-}$mutant cells. Similar to **PFT-α**,[26] analogues **4b** and **2b** did not prevent p53 phosphorylation on the S_{15} residue (data not shown). We therefore used p21/WAF1 increased protein levels as a read-out to evaluate the effects of

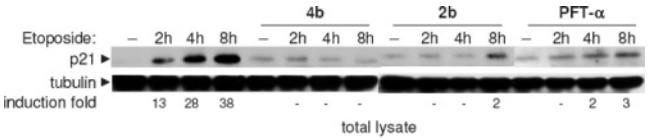

Figure 5. Time course experiment to assay the abilities of **4b** (300 nM), **2b** (3 μM) and **PFT-α** (3 μM) to prevent p21/WAF1-increased protein levels.

the studied compounds on p53 transcriptional activity. Compounds **4b** and **2b** prevented p53-triggered increase in protein levels of p21/WAF1 similar to that in **PFT-α** (Figure 5), indicating that these analogues behaved as p53 posttranscriptional activity inhibitors.[16]

Performing time course as well as concentration-dependent experiments, we found that lower concentrations of **4b** (30 nM) were sufficient to prevent the increase of p21/WAF1 levels compared to those in **PFT-α** and **2b**, which required higher concentrations (300 nM) to induce the same effect (data not shown). Altogether, these results indicate that **4b** efficiently blocks p53-triggered cell death and p21/WAF1 expression in cortical neurons exposed to etoposide at concentrations one order magnitude lower than that in **PFT-α**.

Evaluation in Vivo. We next examined whether **2b** and **4b** could suppress p53-dependent neuronal death in vivo. For these studies, we analyzed the survival of retinal ganglion cells (RGCs) in the paradigm of axotomy-induced apoptotic cell death. The phosphorylation of p53 on the S_{15} residue occurs at day 1 after optic nerve transection with a peak at day 4 in the RGC layer and returns to control levels at day 7 post axotomy. The p53 phosphorylation correlates with a protracted upregulation of p21/WAF1 expression with a peak at day 7 after optic nerve axotomy (data not shown). These results show that p53 plays an important role in neuronal death in this model. We assayed the survival of RGCs after the intravitreal treatment with **2b**, **4b,** and **PFT-α**. Both **4b** and **2b** inhibitors were well tolerated in rats after intraocular injections, as has been previously reported for **PFT-α** after injection in mice.[28] The intraocular administration of **PFT-α** resulted in the increased survival of RGCs at a concentration of 6 μM (131 $\pm$ 27%) but not at 0.06 μM (98 $\pm$ 15%), relative to that of the vehicle control (100 $\pm$ 18%) (Figure 6).

Remarkably, **2b** already showed significant protective effects on RGCs at 0.06 μM (150% $\pm$ 5). In contrast, **4b** was not effective in vivo, even at 6 μM. These studies clearly show that cyclic analogue **4b**, the most active compound in vitro, does not show any activity in vivo. In contrast, the corresponding open compound **2b** is as efficient as **PFT-α** in preventing cell death in vitro but two log values more active in vivo. To explain these in vivo observations, we then performed stability and degradation studies of compounds **2b** and **4b**.

Stability and Degradation Studies. In contrast to ketone analogue **2b**, which could be cyclized into its corresponding analogue **4b** (Scheme 2), oxime analogue **2g**, known as a stable protecting group in various conditions (acido-basic media, aqueous, or different organic solvents),[29] cannot be cyclized. Recall that **2g** was found to be inactive in preventing p53-induced death in vitro (Figure 3), indicating that the ability of open compounds to undergo the cyclization process is an essential feature for inhibitory activity (Figure 3).

Compounds **2b**, **4b,** and oxime **2g** stabilities were next assayed in different media: ethanol/H_2O, serum, or neurobasal culture media. Using an NMR technique, we found that **2b** was converted into **4b** when incubated in chemical and/or biological

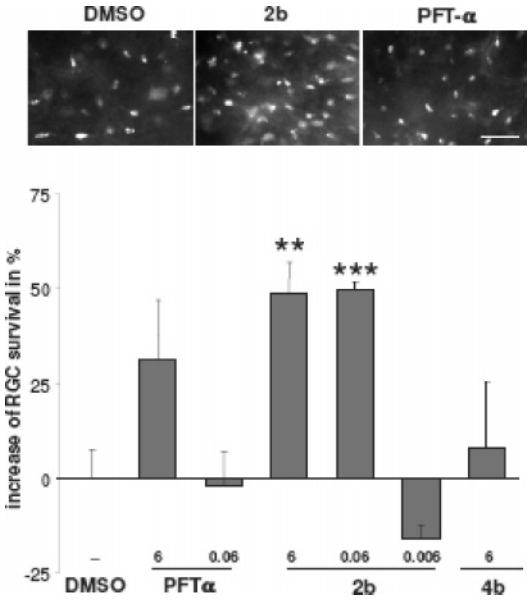

Figure 6. Upper panel: representative areas of flat mounted middle retinal diameters after intraocular injections of DMSO, **2b** (0.06 μM), and **PFT-α** (0.06 μM) showing RGC after staining with FluoroGold. Bar = 40 μm. Lower panel: increased RGC survival after treatment with p53 inhibitors. RGC numbers in DMSO injected animals are set to zero. Intraocular injection of **PFT-α** slightly increased survival of RGC at the concentration of 6 μM but not at 0.06 μM. p53 inhibition only partially restored RGC levels, indicating that RGC degeneration is also controlled by p53-independent pathways. Compound **2b** showed significant protective effects on RGC survival at 0.06 μM, whereas **PFT-α** was only active at 6μM, and compound **4b** was not effective in vivo. RGC counts are given at the inner retinal diameters. All data is given as mean $\pm$ sem. $p < 0.01$ (**); $p < 0.001$ (***).

media. We also found by analytical chromatography that the degradation process of **2b** was negligible. Indeed, **2b** was only converted into its corresponding cyclic derivative **4b** ($t_{1/2}$ = 8 h $\pm$ 0.5) when incubated in biological conditions (data not shown). Consistent with our data, the same cyclization process has been recently reported for **PFT-α**.[21,30] Interestingly, the longer preincubation time of **2b** in biological media significantly increased its inhibitory activity.

As expected, oxime derivative **2g** was found to be very stable after incubation in the same biological media for more than 2 days. In contrast, cyclic compound **4b** was no longer detected after 24 h of incubation, and its half-life ($t_{1/2}$ = 6 h $\pm$ 0.5) was higher than that of **PFT-α** ($t_{1/2}$ = 4 h $\pm$ 0.5).

It should be emphasized that we never observed the retroconversion of cyclic compound **4b** into its open analogue **2b**, confirming that the observed dehydration is an irreversible process. These results show that open form **2b** should be transformed, in situ, into its cyclic form **4b** to become active. Thus, **2b** can be viewed as a prodrug of **4b**. Open form **2b**, allows the generation over the time of the cyclic active form **4b**. A stationary state occurred, during which a sufficient concentration of **4b** remained present to allow an efficient p53 inhibition in vivo.

We next analyzed the stability of **4b** when incubated in different experimental conditions: in ethanol/H_2O solution or in horse serum for 1 or 24 h. Compound **4b** showed a characteristic absorption at λ_{max} = 323 nm in ethanol/H_2O solution. After 24 h of incubation in horse serum, a total disappearance of this peak was observed, suggesting that no more free **4b** was present in the incubation media. In contrast, a new absorption peack appeared at λ_{max} = 398 nm, indicating that new products were formed. Because the incubation biologi-

Scheme 2[a]

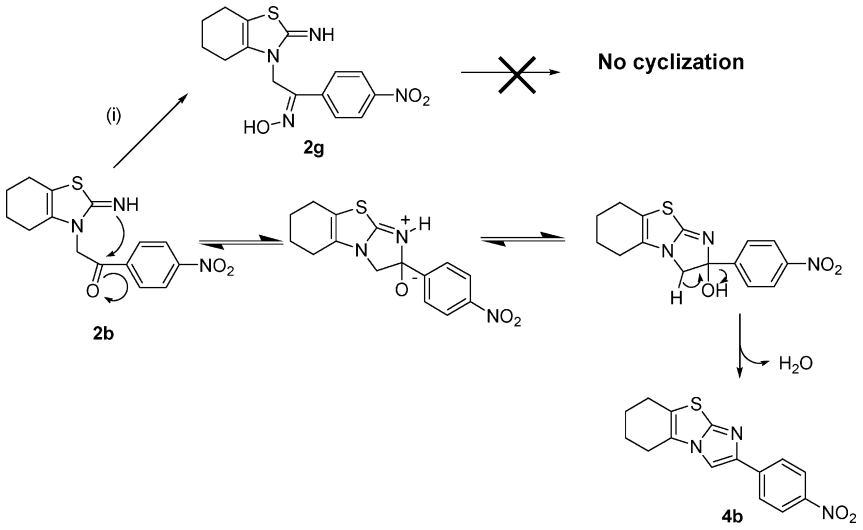

[a] (i) NH_2-OH, **2b**, CH_2Cl_2, 3 h; **2g** (35%).

cal media contained several reactive moieties (free amino acids and proteins), we hypothesized that biological species could react with **4b** to form new adducts.

The disappearance of **4b** in the biological condition could explain the observed loss of in vivo activity. It could also be possible that during the time taken (4 days) because of low solubility a deposition of active compound **4b** in biological conditions could occur in vivo.

Conclusion

The presented mechanistic studies as well as the stability studies support the hypothesis that cyclic compound **4b** could be the active form generated over time from its corresponding open precursor **2b**, which acts as a prodrug precursor. Indeed, longer **2b** preincubation time in the biological assay enhanced its in vitro inhibitory activity. Moreover, the noncyclizable oxime analogue **2g**, inactive in blocking p53-induced death, confirms the requirement of cyclic analogues for p53 inhibition. Open form **2b** being more stable than its cyclic analogue **4b**, slowly released this later and remained active until its reaction with the alkylating species present in biological media. Thus, the increased availability of **2b** over time is likely to ensure a prolonged p53 inhibition after injection in vivo, which is an essential feature for possible therapeutic application. These results support the finding that a subtle balance between the open prodrug precursor and the cyclic active form of the imino-tetrahydrobenzothiazole analogues regulates their inhibitory activity in vivo. Issues of potency and efficacy of this scaffold as p53 inhibitors have to take into account this slow kinetic of intramolecular cyclization to design analogues that could be attractive drugs for in vivo therapeutic perspectives.

The identification of open analogue **2b**, a two log values more active p53 inhibitor than reference p53 inhibitor **PFT-α** in vivo, and its action mechanism studies strengthen the interest to develop novel p53 inhibitors based on the imino-tetrahydrobenzothiazole scaffold with reduced cyclization kinetics. Further studies are needed to address their true therapeutic potential. This strategy may be applicable not only to block p53-triggered death but may result in more effective treatments when combined with the trophic support provided by survival signals.

Experimental Section

Chemistry. Unless otherwise noted, starting materials and reagents were obtained from commercial suppliers and were used without purification. Tetrahydrofuran (THF) was distilled over sodium benzophenone ketyl immediately prior to use. Methylene dichloride (CH_2Cl_2) was distilled over P_2O_5 just prior to use. Toluene and dimethylformamide (DMF) were of anhydrous quality from commercial suppliers (Aldrich, Acros, Carlo Erba Reagents). Nuclear magnetic resonance spectra were recorded at 250 MHz for ^{1}H and 62.9 MHz for ^{13}C on a Brüker AC-250 spectrometer. Chemical shifts are expressed as δ units (part per million) downfield from TMS (tetramethylsilane). Electro-spray mass spectral analysis and LC-MS analysis were obtained on a Waters Micromass ZMD spectrometer for the ES-MS analysis by direct injection of the sample solubilized in acetonitrile. The LC-MS analysis was carried out by using a Waters model 2690 pump and a Waters C18 Symmetry column with a two-mobile phase system (0.1% formic acid in water and 0.1% formic acid in acetonitrile). Microanalyses were carried out by Service Central d'Analyses du CNRS (Venaison, France) and were within 0.4% of the theoretical values. Analytical thin layer chromatographies (TLC) and preparative thin layers chromatographies (PLC) were performed using silica gel plates 0.2 mm thick and 1 mm thick, respectively (60F254 Merck). Preparative flash column chromatographies were carried out on silica gel (230−240 mesh, G60 Merck). The melting points were not determined because of the amorphous character of our peptides and derivatives.

Synthesis of 2-Aminothiazole Hydroiodide Salts Derivatives. General Procedure I. A mixture of ketone (20.0 mmol, 1.0 equiv), thiourea (40.0 mmol, 2.0 equiv) and iodine (20.0 mmol, 1.0 equiv) was stirred at 110 °C for 12 h. The reaction mixture was cooled to room temperature. Hot water (20 mL) was then added to solubilize the crude material, and the resulting solution was stirred for 30 min. The aqueous solution was washed with diethyl ether and then neutralized by the addition of solid $NaHCO_3$. The pale yellow crystals were collected by filtration and identified without any further purification as the expected compound.

2-Amino-4,5,6,7-tetrahydrobenzothiazole Hydroiodide Salt (1a). The title compound was obtained by condensation of cyclohexanone with thiourea according to general procedure I. Yield: 57%. Mp = 185−187 °C. ^{1}H NMR (DMSO-*d*6) δ 2.50−2.48 (m, 4 H), 1.78−1.75 (m, 4 H). MS-ES *m*/*z* 283 $(M + H)^+$.

2-Amino-5,6,7,8-tetrahydro-4H-cycloheptathiazole Hydroiodide Salt (1b). The title compound was obtained by condensation of cycloheptanone with thiourea according to general procedure I. Yield: 52%. Mp = 110 °C. ^{1}H NMR (DMSO-*d*6) δ 8.2 (s, 2 H), 2.65−2.50 (m, 4 H), 1.74 (m, 6 H). MS-ES *m*/*z* 297 $(M + H)^+$.

2-Amino-4,4a,5,6,7,8,8a,9-octahydro-naphtho[2,3-d]thiazole Hydroiodide Salt (1c). The title compound was obtained by

condensation of decalone with thiourea according to general procedure I. Yield: 55%. Mp = 58 °C. ^{1}H NMR (DMSO-*d*6) δ 6.40 (s, 2 H), 1.20−2.50 (m, 14 H). (M + H$^+$)=336. MS-ES *m*/*z* 337 (M + H)$^+$.

Synthesis of 2-Aminothiazole Derivatives. **General Procedure II.** The previous 2-aminothiazole hydroiodide salt derivative was dissolved in a hot saturated aqueous solution of Na_2CO_3 (20 mL). After cooling, the aqueous solution was extracted with CH_2Cl_2 (3 × 20 mL). The organic layer was dried over anhydrous $MgSO_4$, filtered, and concentrated under reduced pressure. The desired compound was purified by flash chromatography to yield the desired compound as an oil, which was solidified by trituration in diethyl ether.

2-Amino-4,5,6,7-tetrahydrobenzothiazole (3a). The title compound was obtained according to general procedure II. Yield: 92%. *Rf* 0.35 (toluene/EtOAc 3:1). Mp = 38 °C. ^{1}H NMR (DMSO-*d*6) δ 6.40 (s, 2 H), 1.20−2.50 (m, 14 H). MS-ES *m*/*z* 155 (M + H)$^+$.

2-Amino-4,4a,5,6,7,8,8a,9-octahydro-naphtho[2,3-d]thiazole (3b). The title compound was obtained according to general procedure II. Yield: 87%. *Rf* 0.30 (toluene/EtOAc 3:1). Mp = 36 °C. ^{1}H NMR (DMSO-*d*6) δ 5.3 (s, 2 H), 1.20−2.50 (m, 14 H). MS-ES *m*/*z* 209 (M + H)$^+$.

2-Amino-5,6,7,8-tetrahydro-4H-cycloheptathiazole (3c). The title compound was obtained according to general procedure II. Yield: 90%. *Rf* 0.35 (toluene/EtOAc 3:1). Mp = 35 °C. ^{1}H NMR (DMSO-*d*6) δ 5.2 (s, 2 H), 2.65−2.50 (m, 4 H), 1.74 (m, 6 H). MS-ES *m*/*z* 169 (M + H)$^+$.

Preparation of 2-Iminothiazole Derivatives. **General Procedure III.** A mixture of the previous 2-aminothiazole derivative (1.0 mmol, 1.0 equiv) and α-bromomethyl ketone (1.0 mmol, 1.0 equiv) were solubilized in anhydrous toluene (20 mL). The reaction mixture was stirred at room temperature for several hours while the desired compound precipitated as an hydrobromide salt. The precipitate was then filtered from the reaction mixture, washed with a small amount of toluene, and recrystallized from either MeOH/EtOAc or EtOH/EtOAc.

1-(4-Methylphenyl)-2-(4,5,6,7-tetrahydro-2-imino-3(2*H*)-benzothiazolyl)ethanone Hydrobromide Salt (1) (PFT-α). The title compound was obtained according to general procedure III. Yield: 54%. Mp = 256−257 °C. 1H NMR (250 MHz, DMSO-d_6) δ 9.60 (s, 1 H), 7.95 (d, 2 H, *J* = 8.2 Hz), 7.45 (d, 2 H, *J* = 8.2 Hz), 5.70 (s, 2 H), 2.51−2.31 (m, 5 H), 1.83−1.79 (m, 2 H), 1.36 (br s, 1 H), 1.02 (d, 3 H, *J* = 6.5 Hz). ES/MS *m*/*z* 287 (M + H)$^+$.

1-(4-Methoxyphenyl)-2-(4,5,6,7-tetrahydro-2-imino-3(2*H*)-benzothiazolyl)ethanone Hydrobromide Salt (2a). The title compound was obtained according to general procedure III. Yield: 61%. Mp = 205 °C (EtOH/EtOAc). ^{1}H NMR (250 MHz, DMSO-d_6) δ 9.47 (s, 1 H), 8.03 (d, 2 H, *J* = 8.9 Hz), 7.16 (d, 2 H, *J* = 8.9 Hz), 5.67 (s, 2 H), 3.89 (s, 3 H), 2.55 (m, 2 H), 2.32 (m, 2 H), 1.73 (m, 4 H). ESM/MS *m*/*z* 303 (M + H)$^+$.

1-(4-Nitrophenyl)-2-(4,5,6,7-tetrahydro-2-imino-3(2*H*)-benzothiazolyl)ethanone Hydrobromide Salt (2b). The title compound was obtained according to general procedure III. Yield: 55%. Mp = 240 °C (MeOH/EtOAc). ^{1}H NMR (250 MHz, DMSO-d_6) δ 9.54 (s, 1 H), 8.46 (d, 2 H, *J* = 8.9 Hz), 8.28 (d, 2 H, *J* = 8.9 Hz), 5.80 (s, 2 H), 2.56−2.37 (m, 4 H), 1.74 (m, 4 H). ES/MS *m*/*z* 318 (M + H)$^+$.

1-(4-Methylphenyl)-2-(4,4a,5,6,7,8,8a,9-octahydro-2-imino-3(2*H*)-naphthothiazolyl)ethanone Hydrobromide Salt (2c). The title compound was obtained according to general procedure III. Yield: 80%. Mp = 205 °C (MeOH/EtOAc). ^{1}H NMR (250 MHz, DMSO-d_6) δ 9.71 (s, 1 H), 8.34 (d, 2 H, *J* = 8.9 Hz), 8.18 (d, 2 H, *J* = 8.9 Hz), 5.80 (s, 2 H), 2.61−1.20 (m, 17 H). ES/MS *m*/*z* 341 (M + H)$^+$.

1-(4-Methoxyphenyl)-2-(4,4a,5,6,7,8,8a,9-octahydro-2-imino-3(2*H*)-naphthothiazolyl)ethanone Hydrobromide Salt (2d). The title compound was obtained according to general procedure III. Yield: 41%. Mp = 190 °C (EtOH/EtOAc). ^{1}H NMR (250 MHz, DMSO-d_6) δ 9.47 (s, 1 H), 8.03 (d, 2 H, *J* = 8.9 Hz), 7.16 (d, 2 H, *J* = 8.9 Hz), 5.67 (s, 2 H), 3.89 (s, 3 H), 2.55−1.25 (m, 14 H). ES/MS *m*/*z* 357 (M + H)$^+$.

1-(4-Nitrophenyl)-2-(4,4a,5,6,7,8,8a,9-octahydro-2-imino-3(2*H*)-naphthothiazolyl)ethanone Hydrobromide Salt (2e). The title compound was obtained according to general procedure III. Yield: 47%. Mp = 239−240 °C (MeOH/EtOAc). ^{1}H NMR (250 MHz, DMSO-d_6) δ 9.71 (s, 1 H), 8.34 (d, 2 H, *J* = 8.9 Hz), 8.18 (d, 2 H, *J* = 8.9 Hz), 5.80 (s, 2 H), 2.61−1.20 (m, 14 H). ES/MS *m*/*z* 372 (M + H)$^+$.

1-(4-Methylphenyl)-2-(5,6,7,8-tetrahydro-2-imino-4H-cycloheptathiazolyl)ethanone Hydrobromide Salt (2f). The title compound was obtained according to general procedure III. Yield: 61%. Mp = 175 °C. (EtOH/EtOAc). ^{1}H NMR (250 MHz, DMSO-d_6) δ 9.60 (s, 1 H), 7.95 (d, 2 H, *J* = 8.2 Hz), 7.45 (d, 2 H, *J* = 8.2 Hz), 5.22 (s, 2 H), 2.65−2.50 (m, 7 H), 1.74 (m, 6 H). ES/MS *m*/*z* 301 (M + H)$^+$.

2-(4-Nitro-phenyl)-2-(4,5,6,7-tetrahydro-2-imino-3(2*H*)-benzothiazolyl)ethanone Oxime, Hydrobromide Salt (2g). A mixture of NH_2-OH (10 mmol, 1 equiv) and **2b** (10 mmol, 1 equiv) was stirred for 3 h in CH_2Cl_2 (70 mL) at room temperature. The title compound was obtained after filtration and recristalization in AcOEt/MeOH (3:1). Yield: 35%. Mp = 235 °C. ^{1}H NMR (250 MHz, DMSO-d_6) δ 9.65 (s, 1 H), 8.18 (d, 2 H, *J* = 8.9 Hz), 7.93 (d, 2 H, *J* = 8.9 Hz), 6.10 (s, 2 H), 2.56−2.37 (m, 4 H), 2.12 (br, 1 H), 1.74 (m, 4 H). ES/MS *m*/*z* 413 (M + H)$^+$.

Preparation of 2-Iminothiazole Derivatives. **General Procedure IV.** The corresponding hydrobromide salt was stirred in MeOH at room temperature for 6 h or in a biological medium at 37 °C for 6 h. The medium was concentrated and extracted with CH_2Cl_2 after evaporation, and the compound was purified by chromatography.

2-(4-Methylphenyl)imidazo[2,1-b]-5,6,7,8-tetrahydrobenzothiazole (4) (PFT-β). The title compound was obtained according to general procedure IV. ^{1}H NMR (250 MHz, DMSO-d_6) δ 7.95 (d, 2 H, *J* = 8.2 Hz), 7.45 (d, 2 H, *J* = 8.2 Hz), 7.3 (s, 1 H), 2.51−2.31 (m, 5 H), 1.83−1.79 (m, 2 H), 1.36 (br s, 1 H), 1.02 (d, 3 H, *J* = 6.5 Hz). ES/MS *m*/*z* 269 (M + H)$^+$.

2-(4-Nitrophenyl)imidazo[2,1-b]-5,6,7,8-tetrahydrobenzothiazole (4b). The title compound was obtained according to general procedure IV. Yield: 55%. Mp = 240 °C. ^{1}H NMR (250 MHz, DMSO-d_6) δ 7.65 (d, 2 H, *J* = 8.5 Hz), 7.45 (s, 1 H), 7.15 (d, 2 H, *J* = 8.5 Hz), 2.40−2.50 (m, 4 H), 1.80−1.95 (m, 4 H). ES/MS *m*/*z* 300 (M + H)$^+$

2-(4-Nitrophenyl)imidazo[2,1-b]- 4,4a,5,6,7,8,8a,9-octahydronaphthothiazole (4e). The title compound was obtained according to general procedure IV. Yield: 30%. Mp = 211 °C. ^{1}H NMR (250 MHz, DMSO-d_6) δ 7.65 (d, 2 H, *J* = 8.5 Hz), 7.45 (s, 1 H), 7.15 (d, 2 H, *J* = 8.5 Hz), 2.55−1.25 (m, 14 H). ES/MS *m*/*z* 354 (M + H)$^+$.

Stability Assay. The stability of compounds was established according to the following procedure. First, the compounds were incubated in the same biological conditions used to evaluate the inhibitory activity on cortical neurons (37 °C; neurobasal medium + B27 + glutamate). Then, the extraction of the biological medium was performed with methylene chloride, and after solvent evaporation, the residue was analyzed by NMR. The disappearance of the Hb (5.4 ppm) proton in open form **2b** as well as the appearance of the Ha proton (7.3 ppm) in corresponding cyclic form **4b** allowed us to characterize both the structure and half-lives of the two analogues during in situ conversion.

Antibodies and Reagents. The antibodies used were anti-tubulin (Sigma), anti-phospho p53 (Cell Signaling), and anti-p21 (Santa Cruz) and Cy-3 labeled anti-rabbit (Dianova, Hamburg, Germany). Etoposide (Sigma) was used at the concentrations indicated in the figure legends. No toxic effects were observed at the concentrations used.

Cortical Neuron Culture and Mice. Cortical neuron cultures were performed according to the following procedure. Neocortices were removed from 15 day-old wild-type or *p53*$^{-/-}$ mutant mouse embryos and digested with trypsin-EDTA for 15 min at 37 °C. Cortical neurons were washed twice with a DMEM/F-12 medium supplemented with 10% horse serum (DMEM/HS), once with a neurobasal medium supplemented with a B27 nutrient (NB/B27,

50:1) (all from Invitrogen), and were then dissociated with a fire-polished glass Pasteur pipet. For biochemistry, the dissociated cells were seeded on poly-DL-ornithine (poly-O, Sigma)-coated 6 cm diameter dishes (Falcon) at a density of 6×10^6/dish in DMEM/HS. Four hours later, the medium was replaced by NB/B27. The cells were cultured for 3 days (3DIV). Electroporation of cortical neurons was performed as previously described.[25] All mice were kept at the IBDM animal facilities, and all experiments were performed in accordance with institutional guide lines.

Survival Assays. Compounds were assessed for their ability to protect cortical neurons against etoposide (1.25 and 2.5 μM) alongside DMSO, and etoposide alone was used as the control. Cells were plated in 96-well plates. Th living cells were visualized using AM-calcein; 10 μL of calcein (1/24) was added per well, and 45 min after incubation, 15 μL of a solution of hemoglobin in PBS (100 mg/mL) was used to quench the reaction. Images of the whole wells were captured using a Flash Cytometer plate reader. The number of surviving cells was automatically evaluated by TYNA software. All experiments were done at least six times. No toxicity of compounds was found at 10 μM. For TUNEL staining, electroporated cortical neurons were fixed with 4% PFA 40 h after electroporation. Following permeabilization with 0.1% Triton X-100, TUNEL was performed according to manufacturer's instructions (Apoptag, In situ apoptosis detection kit, Serologicals Corp.). Cover slips were mounted in Vectashield/Dapi (Vector). All assays were performed in triplicate.

Western Blot Analysis. Total extracts were prepared using boiling total protein extraction buffer (TPEB: 1 part of 10% SDS, 1 part of 1M Tris HCl at pH 6.8, 2 parts of water). Then, sonication and protein determination were performed. Western blots were done as previously described.[31]

Axotomy of the Optic Nerve, Retrograde Labeling, and Animal Numbers. Optic nerve transection was performed as previously described.[32] In brief, adult male Wistar rats (300−400 g; Charles River, Sulzfeld, Germany) were anesthetized by intraperitoneal injection of chloral hydrate (420 mg/kg body weight). The skin was incised close to the superior orbital rim, and the orbita were opened leaving the supraorbital vein intact. The lacrimal gland was moved aside, the superior extraocular muscles detached from their tendinous insertion points, and the eye rotated to expose the optic nerve. The optic nerve was exposed by longitudinal incision of the perineurium and then transected ~2 mm from the posterior eye pole without damaging the retinal blood supply. A 1 × 1 mm piece of gel foam was soaked in FluoroGold (FG; 5% dissolved in 0.9% NaCl; Fluorochrome Inc., Englewood, CO) and placed on the optic nerve stump to retrogradely label retinal ganglion cells. The retinal blood supply was verified by fundoscopy, and animals with persistent retinal ischemia were excluded. For RGC counts, a total of 26 animals were used, with a minimum of $n = 3$ per experimental group: control (DMSO 2%), $n = 6$; **PFT-α** 6 μM and 0.06 μM, $n = 3$ each; **2b** 6 μM and 0.06 μM, $n = 4$ each; 0.006 μM, $n = 3$; **4b** 6 μM, $n = 3$. For immuno-histological visualization of protein regulation, two animals were operated on for each condition, and the contra-lateral eyes served as nonaxotomized controls. All animal experiments were carried out according to the regulations of the local animal research council and state legislation.

Intraocular Drug Administration. Intravitreal injections of p53-inhibitors and vehicles were performed on day 0, 3, and 7 following axotomy. Prior to injection, the animals were briefly anesthetized with diethyl ether. Using a glass micropipet, 3 μL of the inhibitor or vehicle (DMSO 2%) were injected into the vitreous space. The sclera was punctured ~1 mm away from the cornea−sclera junction with the tip of the pipet directed toward the posterior eye pole, taking care not to injure the lens. Animals with cataractogenic lens injury were excluded from the study because lens injury has been shown to have protective effects on RGC survival.

Retinal Flat Mounts and Cell Counting. For RGC survival assays, the animals received an overdose of chloral hydrate, and the eyes were extracted on day 14 post axotomy. The cornea, lens, and the vitreous body were removed, and the remaining eye cup containing the retina was fixed in 4% para-formaldehyde (Sigma) for 1 h. The retinas were then extracted and flat mounted in glycerol−PBS (1:1) on glass slides. The number of FG-positive RGCs was determined by fluorescence microscopy (Zeiss-Axioplan, Oberkochen, Germany) using a UV filter (365/420 nm). Three fields of 62 500 μm^2 were counted in each retinal quadrant at eccentricities of 1/6 (I, inner), 3/6 (M, middle), and 5/6 (O, outer) of the retinal radius. The RGC counts were performed by two different investigators according to a blind protocol.

Immunohistochemistry. For protein expression studies, the animals were sacrificed on day 1, 4, or 7 post axotomy by injecting a chloral hydrate overdose, and the eyes were extracted. The cornea, lens, and the vitreous body were removed, and the remaining eye cup containing the retina was fixed in 4% para-formaldehyde for 1 h. The eye cups were then dehydrated in 30% sucrose at 4 °C for 24 h and immersed in cryostat mounting liquid at −20 °C. Retinal sections of 16 μm were prepared using a Leica cryostat, collected on gelatin-coated glass slides and stored at −20 °C. Tissue sections were dehumidified at 37 °C for 1 h, and antigen retrieval was performed for 4 h in Tris-buffered saline (TBS; pH 9,0) at 60 °C. Unspecific binding was blocked by the application of 10% goat serum, and primary antibodies were applied in a 1:100 dilution at 4 °C overnight. Secondary antibody was then applied for 45 min at room temperature. The sections were then nuclear counter-stained with DAPI (Sigma-Aldrich, Munich, Germany) and mounted in Moviol (Hoechst, Frankfurt, Germany). All comparable images of a series were taken using identical exposure times. Adjustments for brightness and contrast were performed using Corel Draw 8 in an identical manner for all comparable images of one series.

Statistical Analysis. All data is given as mean ± sem. The values were compared using one-way ANOVA and considered as significantly different at $p < 0.05$.

Acknowledgment. We greatfully acknowledge Innate Pharma (Marseille, France), H. Hassani, and T. Drenth for helpful discussions and K. Dudley for the critical reading of the manuscript. We also thank G. Quéléver, C. Garino, Y. Laras, and V. Moret for helpful discussions regarding the synthesis of the new compounds and S. Candeias for p53 mutant mice, R. Demoulin and D. Michel for administrative assistance, and S. Corby and L. Bardouillet for their technical contribution with animal care and genotyping. This work was funded by the "Association Française contre les Myopathies" (AFM), the "Fondation pour la Recherche Médicale" (FRM), the "Association pour la Recherche sur le Cancer" (ARC), the "Fondation de France" (FdF), and the ACI grant. N.P. was supported by INSERM and a "Conseil Régional Provence Alpes Côte d'Azur" fellowship, A.M. by "Ligue contre le cancer" fellowships, and R.D. by a grant from "FRM" and from the Marie Curie Host Fellowship for the Transfer of Knowledge (MTKD-CT-2004-509804).

Supporting Information Available: Elemental analysis of compounds. This material is available free of charge via the Internet at http://pubs.acs.org.

References

(1) Jenner, P.; Olanow, C. W. Understanding cell death in Parkinson's disease. *Ann. Neurol.* **1998**, *44*, S72−84.
(2) Dirnagl, U.; Iadecola, C.; Moskowitz, M. A. Pathobiology of ischaemic stroke: an integrated view. *Trends Neurosci.* **1999**, *22*, 391−397.
(3) Mattson, M. P. Apoptosis in neurodegenerative disorders. *Nat. Rev. Mol. Cell. Biol.* **2000**, *1*, 120−129.
(4) Green, V. J.; Kokkotou, E.; Ladias, J. A. Critical structural elements and multitarget protein interactions of the transcriptional activator AF-1 of hepatocyte nuclear factor 4. *J. Biol. Chem.* **1998**, *273*, 29950−29957.
(5) Blum, D.; Wu, Y.; Nissou, M. F.; Arnaud, S.; Alim Louis, B.; Verna, J. M. p53 and Bax activation in 6-hydroxydopamine-induced apoptosis in PC12 cells. *Brain Res.* **1997**, *751*, 139−142.

(6) Sakhi, S.; Bruce, A.; Sun, N.; Tocco, G.; Baudry, M.; Schreiber, S. S. Induction of tumor suppressor p53 and DNA fragmentation in organotypic hippocampal cultures following excitotoxin treatment. *Exp. Neurol.* **1997**, *145*, 81−88.
(7) Xiang, H.; Kinoshita, Y.; Knudson, C. M.; Korsmeyer, S. J.; Schwartzkroin, P. A.; Morrison, R. S. Bax involvement in p53-mediated neuronal cell death. *J. Neurosci.* **1998**, *18*, 1363−1373.
(8) Cregan, S. P.; MacLaurin, J. G.; Craig, C. G.; Robertson, G. S.; Nicholson, D. W.; Park, D. S.; Slack, R. S. Bax-dependent caspase-3 activation is a key determinant in p53-induced apoptosis in neurons. *J. Neurosci.* **1999**, *19*, 7860−7869.
(9) Uberti, D.; Belloni, M.; Grilli, M.; Spano, P.; Memo, M. Induction of tumour-suppressor phosphoprotein p53 in the apoptosis of cultured rat cerebellar neurones triggered by excitatory amino acids. *Eur. J. Neurosci.* **1998**, *10*, 246−254.
(10) Crumrine, R. C.; Thomas, A. L.; Morgan, P. F. Attenuation of p53 expression protects against focal ischemic damage in transgenic mice. *J. Cereb. Blood Flow Metab.* **1994**, *14*, 887−891.
(11) Li, R.; Waga, S.; Hannon, G. J.; Beach, D.; Stillman, B. Differential effects by the p21 CDK inhibitor on PCNA-dependent DNA replication and repair. *Nature* **1994**, *371*, 534−537.
(12) Napieralski, J. A.; Raghupathi, R.; McIntosh, T. K. The tumor-suppressor gene, p53, is induced in injured brain regions following experimental traumatic brain injury. *Brain Res. Mol. Brain Res.* **1999**, *71*, 78−86.
(13) de la Monte, S. M.; Sohn, Y. K.; Wands, J. R. Correlates of p53- and Fas (CD95)-mediated apoptosis in Alzheimer's disease. *J. Neurol. Sci.* **1997**, *152*, 73−83.
(14) Jeffers, J. R.; Parganas, E.; Lee, Y.; Yang, C.; Wang, J.; Brennan, J.; MacLean, K. H.; Han, J.; Chittenden, T.; Ihle, J. N.; McKinnon, P. J.; Cleveland, J. L.; Zambetti, G. P. Puma is an essential mediator of p53-dependent and -independent apoptotic pathways. *Cancer Cell* **2003**, *4*, 321−328.
(15) Moll, U. M.; Wolff, S.; Speidel, D.; Deppert, W. Transcription-independent pro-apoptotic functions of p53. *Curr. Opin. Cell Biol.* **2005**, *17*, 631−636.
(16) Komarov, P. G.; Komarova, E. A.; Kondratov, R. V.; Christov-Tselkov, K.; Coon, J. S.; Chernov, M. V.; Gudkov, A. V. A chemical inhibitor of p53 that protects mice from the side effects of cancer therapy. *Science* **1999**, *285*, 1733−1737.
(17) Culmsee, C.; Zhu, X.; Yu, Q. S.; Chan, S. L.; Camandola, S.; Guo, Z.; Greig, N. H.; Mattson, M. P. A synthetic inhibitor of p53 protects neurons against death induced by ischemic and excitotoxic insults, and amyloid beta-peptide. *J. Neurochem.* **2001**, *77*, 220−228.
(18) Zhu, X.; Yu, Q. S.; Cutler, R. G.; Culmsee, C. W.; Holloway, H. W.; Lahiri, D. K.; Mattson, M. P.; Greig, N. H. Novel p53 inactivators with neuroprotective action: syntheses and pharmacological evaluation of 2-imino-2,3,4,5,6,7-hexahydrobenzothiazole and 2-imino-2,3,4,5,6,7-hexahydrobenzoxazole derivatives. *J. Med. Chem.* **2002**, *45*, 5090−5097.
(19) Duan, W.; Zhu, X.; Ladenheim, B.; Yu, Q. S.; Guo, Z.; Oyler, J.; Cutler, R. G.; Cadet, J. L.; Greig, N. H.; Mattson, M. P. p53 inhibitors preserve dopamine neurons and motor function in experimental parkinsonism. *Ann. Neurol.* **2002**, *52*, 597−606.
(20) Pietrancosta, N.; Maina, F.; Dono, R.; Moumen, A.; Garino, C.; Laras, Y.; Burlet, S.; Quelever, G.; Kraus, J. L. Novel cyclized Pifithrin-alpha p53 inactivators: synthesis and biological studies. *Bioorg. Med. Chem. Lett.* **2005**, *15*, 1561−1564.
(21) Barchechath, S. D.; Tawatao, R. I.; Corr, M.; Carson, D. A.; Cottam, H. B. Inhibitors of apoptosis in lymphocytes: Synthesis and biological evaluation of compounds related to pifithrin-alpha. *J. Med. Chem.* **2005**, *48*, 6409−6422.
(22) Johnson, M.; Lajiness, M.; Maggiora, G. Molecular similarity: a basis for designing drug screening programs. *Prog. Clin. Biol. Res.* **1989**, *291*, 167−171.
(23) Evans, B. E.; Rittle, K. E.; Bock, M. G.; DiPardo, R. M.; Freidinger, R. M.; Whitter, W. L.; Lundell, G. F.; Veber, D. F.; Anderson, P. S.; Chang, R. S.; et al. Methods for drug discovery: development of potent, selective, orally effective cholecystokinin antagonists. *J. Med. Chem.* **1988**, *31*, 2235−2246.
(24) King, L. C.; Hlavacek, R. The reaction of ketones with iodine and thiourea. *J. Am. Chem. Soc.* **1950**, *72*, 3722−3725.
(25) Tulasne, D.; Deheuninck, J.; Lourenco, F. C.; Lamballe, F.; Ji, Z.; Leroy, C.; Puchois, E.; Moumen, A.; Maina, F.; Mehlen, P.; Fafeur, V. Proapoptotic function of the MET tyrosine kinase receptor through caspase cleavage. *Mol. Cell. Biol.* **2004**, *24*, 10328−10339.
(26) Thompson, T.; Tovar, C.; Yang, H.; Carvajal, D.; Vu, B. T.; Xu, Q.; Wahl, G. M.; Heimbrook, D. C.; Vassilev, L. T. Phosphorylation of p53 on key serines is dispensable for transcriptional activation and apoptosis. *J. Biol. Chem.* **2004**, *279*, 53015−53022.
(27) Arriola, E. L.; Lopez, A. R.; Chresta, C. M. Differential regulation of p21waf-1/cip-1 and Mdm2 by etoposide: etoposide inhibits the p53-Mdm2 autoregulatory feedback loop. *Oncogene* **1999**, *18*, 1081−1091.
(28) Bae, B. I.; Xu, H.; Igarashi, S.; Fujimuro, M.; Agrawal, N.; Taya, Y.; Hayward, S. D.; Moran, T. H.; Montell, C.; Ross, C. A.; Snyder, S. H.; Sawa, A. p53 mediates cellular dysfunction and behavioral abnormalities in Huntington's disease. *Neuron* **2005**, *47*, 29−41.
(29) Greene, W.; Wunts, P. G. *Protective Groups in Organic Synthesis*, 3rd ed.; John Wiley and Sons: New York, 1999; Vol. 1.
(30) Gary, R. K.; Jensen, D. A. The p53 inhibitor pifithrin-alpha forms a sparingly soluble derivative via intramolecular cyclization under physiological conditions. *Mol. Pharm.* **2005**, *2*, 462−474.
(31) Maina, F.; Pante, G.; Helmbacher, F.; Andres, R.; Porthin, A.; Davies, A. M.; Ponzetto, C.; Klein, R. Coupling Met to specific pathways results in distinct developmental outcomes. *Mol. Cell* **2001**, *7*, 1293−1306.
(32) Kermer, P.; Klocker, N.; Weishaupt, J. H.; Bahr, M. Transection of the optic nerve in rats: studying neuronal death and survival in vivo. *Brain Res. Brain Res. Protoc.* **2001**, *7*, 255−260.

JM060318N